

## AN IMPROVED DILATION METHOD FOR THE MEASUREMENT OF FRACTAL DIMENSION

Siegfried Eins

Institut für Anatomie, Universität Göttingen, Kreuzberggring 36  
D-37075 Göttingen, Germany

### ABSTRACT

According to mathematical foundations of fractal dimensions ( $D$ ) several methods were introduced for the measurement of  $D$ , first as manual techniques, later as computer algorithms. An image analysis environment may be especially appropriate for the automatic measurement of fractal dimensions. With regard to efficiency and accuracy dilation seems to be the most advantageous approach among the known methods (yard stick, box counting, dilation etc.). Unfortunately, there remains one misleading point: while analysing lineal objects with open ends (in contrast to closed contours) the measured  $D$ -values are systematically underestimated. The degree of bias depends on the number of end points and the complexity of a given structure. A method will be presented to avoid this bias by using direction controlled vectorial structuring elements in combination with specially designed anisotropic morphological filters. Applied to a given neuro-anatomical structure (processes of astrocytes)  $D$  is corrected from 1.56 to 1.68. A further application demonstrates the impact of using projection images on measured  $D$ -values.

**Key words:** dilation, fractal dimension, image analysis, neuro-anatomy, software, structuring element.

### INTRODUCTION

The knowledge of fractal dimension ( $D$ ) provides additional structural information about a given structure which is not available from other structural parameters. This explains the strong interest in the development of reliable and easy to use methods for the measurement of  $D$  in very different fields of research ranging from molecular biology and medicine to astronomy and geosciences. For the analysis of length fractals ( $1.0 < D < 2.0$ ) of images it is a convenient technique to evaluate the length of a line, profile, contour, etc. by using different scales or magnifications. In this respect yard stick (Richardson 1961, Mandelbrot 1983) and box counting methods (Barnsley 1993) were most popular and applicable without any computer support. These methods estimate the length ( $P$ ) of a line either by the length of a polygon obtained with different divider steps ( $R$ ), or by counting those boxes of super-imposed rasters of different spacings ( $R$ ) which contain the object. According to Richardson (1961) the  $\log(P) - \log(R)$ -plot of the measured data set allows the evaluation of  $D$  for a given structure by calculating the inclination of the obtained straight curve. Other methods for  $D$ -measurement

have been developed, e.g. intercept censoring (Flook 1982), equi-distant points (Schwarz & Exner 1980), density correlation (Witten & Sander 1981), mass-size relation (Kaye 1989) and dilation (Flook 1978). They operate very similar to the methods mentioned first with minor variations depending on the power law behind the particular method. Reviews may be found in e.g. Clark (1986), Cross (1994), Farin et al. (1985), Kaye (1989), Mandelbrot (1983), Pfeifer & Obert (1989), Rigaut (1990) and Stoyan & Stoyan (1992).

In any case, the multiple measurements at various scales constitute an increased expenditure of time which is a strong argument for the automation of such measurements. The types of processing steps in corresponding algorithms (counting, area and length measurements) give reasons for a successful use of image analysis systems in this field. This has been shown by Eins & Rollmann (1993) for all the methods mentioned before.

This contribution deals with the dilation method for  $D$ -measurements. Flook (1978) already pointed out the usefulness of dilation in combination with automatic image processing for fractal analysis. He also mentioned a source of error coming from a "cap" effect which underestimates  $D$ . It only occurs if the structure to be analysed has open ends. This bias could not be avoided by the former machinery for image analysis.

The end point bias can be corrected or even avoided if the usual "isotropic" structuring elements (octagons, squares) are replaced by specifically designed anisotropic ones. Thus more correct values for  $D$  are obtained also for structures with open ends. This is especially important in neuro-anatomical applications with multiply arborised cell processes and a consequently high number of open ends. Correct data also constitute the basic requirement to critically assess the approach of  $D$ -measurements from projected images (Mandelbrot 1983, Porter et al. 1991).

## MATERIAL AND METHODS

Programs and measurements of this study are related to the IBAS<sup>®</sup>-image analysis system, software release 2.0 (Kontron, Eching). It especially takes advantage of the MDL-tool (Morpho-Definition Language) enabling the user to design arbitrary 3\*3 structuring elements which fulfill a key function in avoiding the end point bias in fractal analysis by dilation.

The structures referred to in this study were different test objects and neuro-anatomical structures studied in this laboratory (Rollmann 1992), namely micrographs of rat astrocytic cell processes and electron-micrographs of the lamellar extrusions found on such processes. The cell processes were obtained by through-focussing of single GFAP (Glial Fibrillary Acidic Protein)-stained cells in thick sections (50 $\mu$ m) and drawing the processes via a camera lucida into one projection image. Then these images were loaded into the measuring system by a tv-camera and skeletonized before analysis (Fig.1B). The lamellar structures were available as 3-dimensional reconstructions from serial sections. The HRP (HorseRadish Peroxydase)-filled glial lamellae were cut out from silicon plates of 1mm thickness corresponding to 50nm-sections and a final 20 000x magnification of the electron micrographs. The assembled reconstructions (Fig.6) were tilted in front of the tv-camera to find out the impact of projection angles on  $D$ -values (Fig.7). For these measurements the contours were extracted from the stored projection images.

**RESULTS**

Considering the advantages of the dilation method for  $D$ -measurement as compared with other methods it appears worth developing dilation as a standard routine method for  $D$ -measurement. However, this approach is restricted by the "cap bias" appearing in connection with open ends of the analysed structures (Flook 1978). In principle, fractal analysis by dilation includes the following steps for different scales  $R$  (number of dilation steps):

- dilate the generating structure (profile, line, contour) by  $R$  using as a rule an "isotropic" structuring element
- evaluate the area  $A$  of the dilated structure
- find a length estimate  $P$  of the original structure as  $A/R$  where  $R$  is the thickness of the band.

Finally, plot these data as  $\log(P)$  vs.  $\log(R)$  (Richardson-plot) and calculate  $D$  from the inclination of the obtained straight line according to the underlying power law

$$P \approx R^{1-D} \tag{1}$$

"Isotropic" structuring elements as used in Fig.1 dilate a closed lineal structure in width (Fig.1A), thus allowing to regard the obtained area as a measure of its length. On the other hand, open ending lines are also dilated in length by addition of semi-"circular" caps at the open ends (Fig.1B). This results in an overestimation of band area  $A$  and, consequently, an overestimation of the length estimate  $P$  by simulating an elongation of the structure at its end points. According to Eq.1 this corresponds to an underestimation of  $D$ . In order to avoid this bias a method must be found to hinder the dilation from extending into the cap region which requires anisotropic structuring elements as explained in Fig.2.

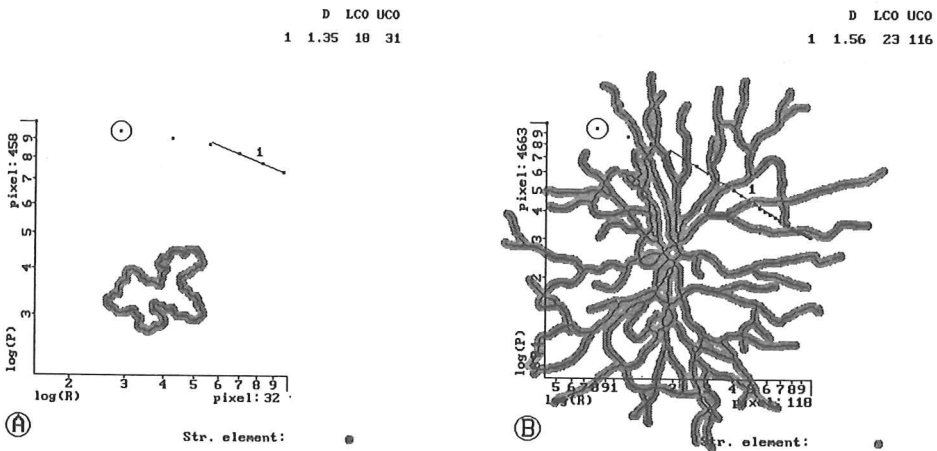


Fig. 1: Richardson-plots of the well documented Medalia particle as a test object (A) and the skeletonised processes of an astrocyte (B). The dilation bands and the size of the octagonal structuring element correspond to an intermediate dilation step marked by the encircled data points. The finally calculated  $D$ -values are given in the top right corners together with the lower (LCO) and upper (UCO) cutoffs of the linear measuring range in pixels.

The MDL-tool offered by the IBAS<sup>®</sup>-system allows to design arbitrary dilation filters including anisotropic ones as long as they can be defined in a 3\*3 matrix or by repetitive applications of such filters. This allows to resolve the problems mentioned and even to avoid the end point bias. MDL-operators are simply defined in ASCII-files. Two examples should demonstrate the principle:

Assume we want to dilate a defined isolated pixel out of a larger pixel set not in the usual way by an "isotropic" structuring element (octagon, square,...) but by a horizontally orientated (dir=0) 90°-sector (Fig.3). In a first part we have to find the generator pixel (A or B in Fig.3) from where the sectorial dilation should start by defining appropriate elements:

$$\begin{array}{ll}
 \text{element findA=} & \begin{matrix} 1 & 0 & 0 \\ 0 & 1 & 0 \\ 1 & 0 & 0; \end{matrix} & \text{element shiftAB=} & \begin{matrix} X & X & X \\ 1 & 0 & X \\ X & X & X; \end{matrix} & (2)
 \end{array}$$

("1", "0" and "X" stand for "hit", "miss" or "either of both", respectively).

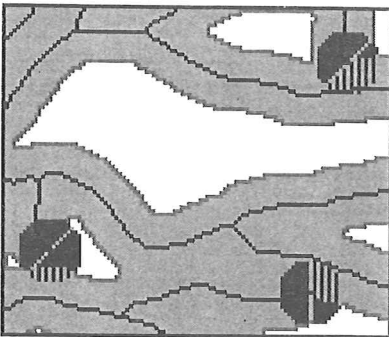


Fig. 2: Enlarged detail of Fig.1B showing the contribution of three end points to "isotropic" dilation. Only the filled part of the outer semi-"circles" constitute the end point bias.

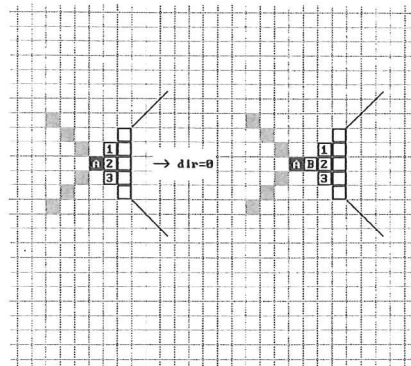


Fig. 3: Explanation of the MDL-tool: a single pixel (A or B) has to be dilated by an anisotropic structuring element with the shape of a horizontal sector. For details see text.

To find B both steps may be serially linked by a sequential operator:

$$\text{sequence findB=} \quad \text{findA shiftAB;} \quad (3)$$

Now the sectorial dilation: We proceed as usual and look at dilation as the inverse of background erosion. Instead of using "0" all around in the eroding element ("isotropical" case) we selectively replace "0" by "X":

$$\begin{array}{ll}
 \text{element erobkgsect=} & \begin{matrix} 0 & X & X \\ 0 & 0 & X \\ 0 & X & X; \end{matrix} & (4)
 \end{array}$$

The final sectorial dilation is obtained by a parallel operation of background erosion and image inversion:

$$\text{parallel dilsect} = \text{not erobksect}; \tag{5}$$

In addition to "not" the parallel operators "and" and "or" are available. They may be nested and combined according to priority rules. The final filter is then called from the program by its name and repetitive applications may be programmed by a count parameter (count=1 finds pixels 1 to 3 in Fig.3 and so forth):

$$\text{morpho3x3 input,output,name,file,count} \tag{6}$$

Analogous to the example shown before in Fig.3 MDL may be used to avoid the "cap bias" associated with open end points (E in Fig.4). The result is shown for this test figure (which must not be fractal). The principle operates as follows: Find for each pixel of the original structure (black) the local direction(s) to which it belongs (by MDL, similar to Eq.2). Dilate each pixel by a vectorial structuring element normal to its directional affiliation (grey pixels in Fig.4; this type of dilation is usually available on image analysis equipment). No bias appears by

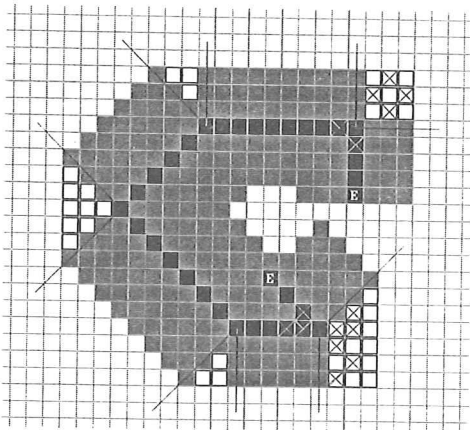


Fig. 4: A model structure (black pixels) with two open ends (E). The effect of orientation sensitive vectorial dilation (grey pixels) and the requirement of additional sectorial dilation (empty pixels) to avoid the end point bias is demonstrated. The angular width of the sectors (45°, 90°, 135°) corresponds to the change in direction at that position of the original structure. For more details see text.

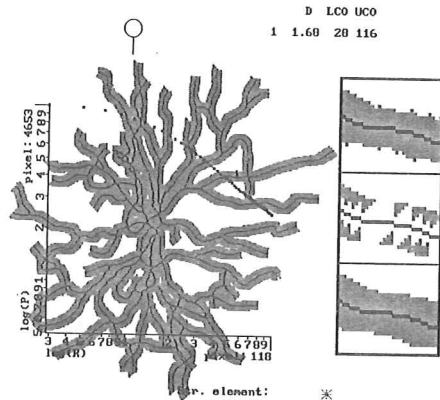


Fig.5: Same structure as in Fig.1B but corrected for end point bias by vectorial dilation subject to local direction and sectorial supplementation. The circle points to the displayed step of dilation. The details (right) give a step by step operation: top - vectorial dilation alone leads to dilation bands with rough envelopes caused by the entity of remaining empty sectors (Fig.4); middle - sectorial supplements for those original pixels where direction changes by 45° (cf. Fig.4); bottom - the "smoothed" sum of both.

exceeding dilation beyond the end points E. Unfortunately, on the convex side of the obtained band, sectors of different angular widths remain undetected (unfilled pixels). The starting points of these sectors are associated with those pixels in the original in which directional changes take place. Directional changes ( $45^\circ$ ,  $90^\circ$  or  $135^\circ$ ) again may be found by MDL-operators (cf. Eq.2 and Fig.3). It is no problem to correct this new bias by dilation with appropriately designed structural elements. Notice the similarity to the operations described in the examples of Fig.3 and Eq.2 to 6: localise pixels of certain characteristic, move them to start positions for sectorial dilation and, lastly, perform the anisotropic dilation according to local orientation and change of direction at this point. The operators show rotational symmetry for different directions (dir in Fig.3) and may be found by rotating the matrices with minor differences for orthogonal and diagonal directions, respectively. In case of  $45^\circ$  and  $135^\circ$ -dilation the 8-connectivity inside the dilation band must be established by another simple MDL-operator as a part of diagonal sectorial dilation. Finally, at the corners some pixels are assigned to artificial directions (X on black) and dilated correspondingly (X on white). However, this artifact affects only pixels which will be hit anyway by sectorial dilation. - End points in the inner part of a structure become embedded by progressive dilation of other parts of the structure in accordance with the intended end point correction.

Applying the new method to the neuro-anatomical example given before the fractal dimension increases from  $D = 1.56$  (Fig.1B) to  $D = 1.68$  (Fig.5).

A further application concerns the possible effect of using projected images for  $D$ -measurements (Mandelbrot 1983, Porter et al. 1991). Fig.6 shows one of the physical 3-dimensional reconstructions of astrocytic lamellae together with a part of a process. The  $D$ -values measured for each viewing direction of the tv-camera are given in Fig.7. The Richardson-plots (Fig.8) displayed three linear parts giving rise to the dimensions  $D_1$ ,  $D_2$  and  $D_3$  from lower to higher scales.  $D_3$  may be assigned to structural fractality of the object itself. The surprising result is a broad plateau for the  $D_3$ -plot meaning that  $D$  is not influenced by the orientation of the projection plane over this angular range. The value found for  $D$  of neuro-anatomical structures (about 1.45 and 1.68, respectively) will not be discussed in this context.

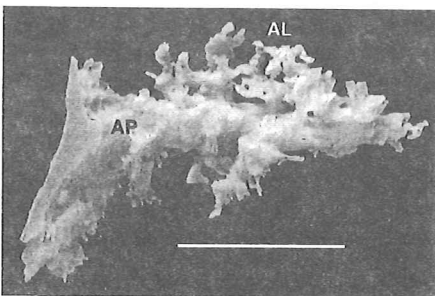


Fig.6: 3d-reconstruction of astrocytic lamellae (AL) around a cell process (AP). Projected images of the lamellae were obtained by tilting these objects (Rollmann 1992) in front of the tv-camera. Scale bar:  $6\mu\text{m}$ .

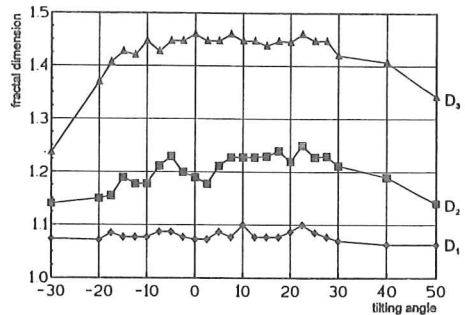


Fig.7: Dimensions  $D$  of reconstructed lamellae at different projection angles as calculated from the linear parts in the Richardson-plots (Fig.8).

Concerning  $D_2$  and  $D_3$  one may suppose that  $D_3$  is an artifact caused by the pixel roughness in digitised images. Similar observations were made in all our measurements (cf. Fig.1, 5).  $D_2$ , on the other hand, seems to be connected with the roughness introduced by the steplike composition from single silicon plates. The disappearance of this part in the Richardson-plots for a viewing angle normal to the plate surface is one argument in favour of this interpretation.

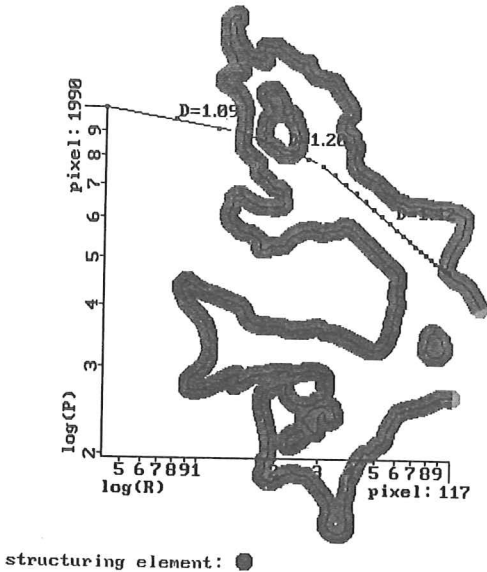


Fig. 8: Lamellar contours as visible in one of the projection planes together with the corresponding Richardson-plot. An inter-mediate dilation pattern is shown obtained by application of an octagonal structuring element. As indicated, the "cap bias" of only two end points has to be corrected.

**DISCUSSION**

The dilation method as well as other image analysis methods developed in our laboratory for  $D$ -measurement were proved by measuring either an arbitrary Euclidian model structure or a deterministic fractal (the Koch curve with known  $D = 1.2619$ ), or the structure shown in Fig.1A which is well documented in the literature ("Medalia particle", cf. Flook 1978, Schwarz 1980, Schwarz & Exner 1980, Farin et al. 1985, Cvijovic & Mihajlovic 1989, Kaye 1989). In any case, the found  $D$ -values correspond to those expected theoretically or known from literature, respectively (Eins & Rollmann 1993).

Dilation has an outstanding role among these methods because it is easy to program on image analysis equipment, the mainly parallel processing makes it running fast and there is no need for any external references. For the other methods we found that results display a certain degree of translational and rotational variance depending on relative position of object and external rasters (box counting, intercept censoring, mass-size relation) or on the respective starting point for divider stepping (equi-distant points and yard stick methods). Pfeifer & Obert (1989) called this phenomenon a "non trivial minimization problem" and it is usually treated by

averaging different raster or starting point positions (e.g. Montague & Friedlander 1989, Morse et al. 1985). On the contrary, this problem is unknown to the continuously working dilation method.

As concerns the measurement speed - a further criterion for the acceptance as a routine method - dilation again is faster than the other methods on the same hardware. Our interpreter software is surely not optimised in this respect and so we need an average time per data point of 0.1min if 10 data points are collected. This is true for closed contours as the Medalia particle in Fig. 1A. If a possible end point bias has to be considered (Fig. 1B, 5, 8) this time increases to 1.4min irrespective of the number of end points.

One might assume that other correction methods for the end point bias are more convenient, e.g. a mathematical correction by introducing a correction term for the dilated Area  $A$  (with  $N$ : countable number of end points;  $R$ : size of an assumed circular cap):

$$-N \frac{\pi R^2}{8} \quad (7)$$

But this would result in an overcorrection according to partial super-imposition of cap area and correctly dilated parts of the generating line (hatched area in Fig.2). For the same reason image analysis correction methods different from that described in this study demand a serial and time consuming processing.

Structuring elements usually contained in commercial image analysis equipment include cross, square and octagon, with increasing isotropy. In the presented method, according to the  $\sqrt{2}$ -length-relation of diagonal and orthogonal vectorial dilations the contribution to the area depends on direction. The width of the dilation band varies slightly depending on the locally prevailing orientations which affects  $D$  by about 0.02 units. This effect may also be observed at end points with directional changes just in the end point region. In such cases the termination of the dilated band deviates from a straight line (Fig.5). We consider the remaining anisotropy by calculating the average size for all directions of the structuring element. Furthermore, we check the local directions of the original structure for equal frequencies and homogeneity of distribution. In this respect the circular transform has been recommended instead of structuring elements (Adler & Hancock 1994). However, as for dilation the open end problem must be solved.

## ACKNOWLEDGEMENTS

Supported by grant 279/6-4-111/88 from the Deutsche Forschungsgemeinschaft. I am grateful to Dr TI Chao for manyfold help in preparing the figures and the manuscript, to R Emme for constructing the tilting device and to G Rübiger for carefully reading and correcting the manuscript.

## REFERENCES

- Adler J, Hancock D. Advantages of using distance transform function in the measurement of fractal dimensions by the dilation method. *Powder Technol* 1994; 78: 191-6.
- Barnsley MF. *Fractals everywhere*. Boston: Academic Press, 1993: 171-95.
- Clark NN. Three techniques for implementing digital fractal analysis of particle shape. *Powder Technol* 1986; 46: 45-52.
- Cross SS. The application of fractal geometric analysis to microscopic images. *Micron* 1994; 25: 101-13.
- Cvijovic Z, Mihajlovic D. The application of fractal dimension in describing the irregular shape of intermetallic phase particles. *Acta Stereol* 1989; 8: 325-30.
- Eins S, Rollmann T. Fractal analysis of complex shape in dendritic cells: an image processing approach. *Anat Anz* 1993; 175 (suppl): 162-3.
- Farin D, Peleg S, Yavin D, Avnir D. Applications and limitations of boundary-line fractal analysis of irregular surfaces: proteins, aggregates and porous materials. *Langmuir* 1985; 1: 399-407.
- Flook AG. The use of dilation logic on the Quantimet to achieve fractal dimension characterisation of textured and structured profiles. *Powder Technol* 1978; 21: 295-8.
- Flook AG. Fractal dimensions: their evaluation and their significance in stereological measurements. *Acta Stereol* 1982; 1: 79-87.
- Kaye BH. Image analysis techniques for characterizing fractal structures. In: Avnir D, ed. *The fractal approach to heterogeneous chemistry. Surfaces, colloids, polymers*. Chichester: John Wiley & Sons, 1989: 55-66.
- Mandelbrot BB. *The fractal geometry of nature*. New York: Freeman & Co, 1983.
- Montague PR, Friedlander MJ. Expression of an intrinsic growth strategy by mammalian retinal neurons. *Proc Nat Acad Sci* 1989; 86: 7223-7.
- Morse DR, Lawton JH, Dodson MM, Williamson MH. Fractal dimension of vegetation and the distribution of arthropod body length. *Nature* 1985; 314: 731-3.
- Pfeifer P, Obert M. Fractals: Basic concepts and terminology. In: Avnir D, ed. *The fractal approach to heterogeneous chemistry. Surfaces, colloids, polymers*. Chichester: John Wiley & Sons, 1989: 11-44.
- Porter R, Ghosh S, Lange GD, Smith jr TG. A fractal analysis of pyramidal neurons in mammalian motor cortex. *Neurosci Lett* 1991; 130: 112-6.
- Richardson LF. The problem of contiguity: an appendix to statistics of deadly quarrels. *Gen Syst Yearb* 1961; 6: 139-87.
- Rigaut JP. Fractal models in biological image analysis and vision. *Acta Stereol* 1990; 9: 37-52.
- Rollmann T. Die strukturellen Voraussetzungen der Astroglia für die Kontrolle über das Neuropil im Neocortex der Ratte: eine morphometrische Studie. *Dissertation Fac Med, Univ Göttingen*: 1992.
- Schwarz H. Two-dimensional feature-shape indices. *Mikroskopie* 1980; 37: 64-7.
- Schwarz H, Exner HE. The implementation of the concept of fractal dimensions on a semi-automatic image analyser. *Powder Technol* 1980; 27: 207-13.

Stoyan D, Stoyan H. *Fraktale - Formen - Punktfelder: Methoden der Geometrie-Statistik*. Berlin: Akademie Verlag, 1992: 17-68.

Witten jr TA, Sander LM. Diffusion-limited aggregation, a kinetic critical phenomenon. *Phys Rev Letters* 1981; 47: 1400-3.